RESEARCH ARTICLE

Andrographolide inhibits intracellular *Chlamydia trachomatis* multiplication and reduces secretion of proinflammatory mediators produced by human epithelial cells

Ziyu Hua[1], Kyla M. Frohlich[2], Yan Zhang[1], Xiaogeng Feng[3], Jiaxing Zhang[1] and Li Shen[2],*

[1]Department of Neonatology, Children's Hospital of Chongqing Medical University, Ministry of Education Key Laboratory of Child Development and Disorders, Chongqing Key Laboratory of Pediatrics, Chongqing, China, 400014, [2]Department of Microbiology, Immunology, and Parasitology, Louisiana State University Health Sciences Center, New Orleans, LA 70112, USA and [3]Biodiscovery, Boston, MA 02132, USA

***Corresponding author:** Department of Microbiology, Immunology, and Parasitology, Louisiana State University Health Sciences Center, New Orleans, LA 70112, USA. Tel: +1-504-568-4076; Fax: +1-504-568-2918; E-mail: lshen@lsuhsc.edu
One sentence summary: Andrographolide plays a dual role in Chlamydia–host interaction to inhibit Chlamydia growth and to reduce the secretion of proinflammatory mediators produced by epithelial cells following Chlamydia infection.
Editor: Dagmar Heuer

ABSTRACT

Chlamydia trachomatis is the most common sexually transmitted bacterial disease worldwide. Untreated *C. trachomatis* infections may cause inflammation and ultimately damage tissues. Here, we evaluated the ability of Andrographolide (Andro), a natural diterpenoid lactone component of *Andrographis paniculata*, to inhibit *C. trachomatis* infection in cultured human cervical epithelial cells. We found that Andro exposure inhibited *C. trachomatis* growth in a dose- and time-dependent manner. The greatest inhibitory effect was observed when exponentially growing *C. trachomatis* was exposed to Andro. Electron micrographs demonstrated the accumulation of unusual, structurally deficient chlamydial organisms, correlated with a decrease in levels of OmcB expressed at the late stage of infection. Additionally, Andro significantly reduced the secretion of interleukin6, CXCL8 and interferon-γ-induced protein10 produced by host cells infected with *C. trachomatis*. These results indicate the efficacy of Andro to perturb *C. trachomatis* transition from the metabolically active reticulate body to the infectious elementary body and concurrently reduce the production of a proinflammatory mediator by epithelial cells *in vitro*. Further dissection of Andro's anti-*Chlamydia* action may provide identification of novel therapeutic targets.

Key words: *Chlamydia trachomatis*; Andrographolide; antibacterial activity; anti-inflammation; green fluorescent protein
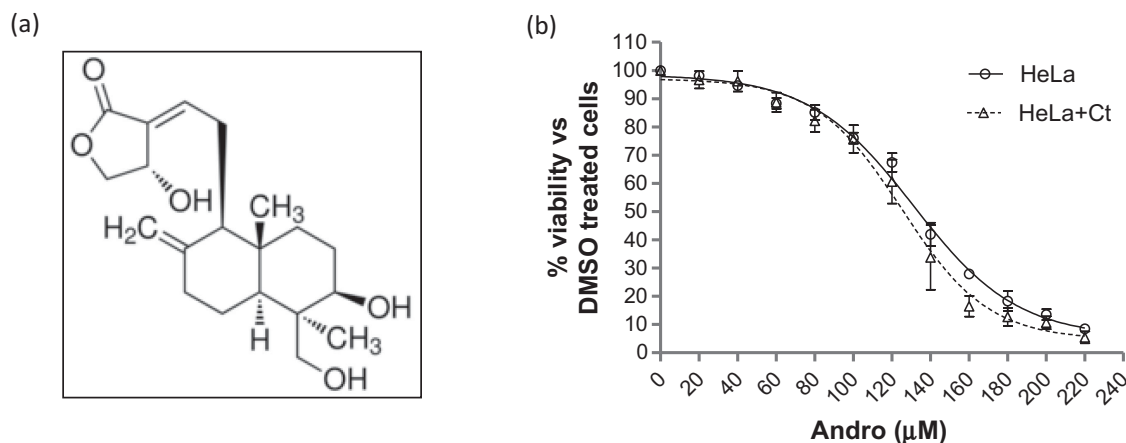
(a)

(b)

Figure 1. Effect of Andro on cell viability of HeLa 229 cells. (**a**) Molecular structure of Andro. (**b**) Cell viability determination using CCK-8 assays. Shown are representative Andro response curves for HeLa 229 cells with (△) and without (○) *C. trachomatis* L2GFP infection (HeLa+Ct). The infected cells were exposed to increasing concentrations of Andro (0–220 μM) for 44 h. The data represent the mean ± SEM. Studies were repeated three times in quadruplicate.

INTRODUCTION

Chlamydia trachomatis is a Gram-negative obligate intracellular bacterium that causes significant public health concerns at a global level (Cohen, Koochesfahani, Meier, *et al.*, 2005; Gottlieb, Brunham, Byrne, *et al.*, 2010). *C. trachomatis* serovars A–C cause trachoma, the leading cause of preventable blindness, while serovars D–K contribute to *Chlamydia*'s place as the most prevalent bacterial sexually transmitted infection (STI) worldwide. Lymphogranuloma venereum (LGV) serovars L1–L3 result in an STI that can become systemic, with symptoms such as ulceration and formation of buboes. Severe reproductive sequelae in women may include the development of pelvic inflammatory disease (PID), tubal scarring, infertility and ectopic pregnancy. Adverse outcomes of *C. trachomatis* infections account for an estimated US$4 billion in healthcare costs per year in the USA alone (Patton, Sweeney and Stamm. 2005; Gottlieb, Brunham, Byrne, *et al.*, 2010). *C. trachomatis* can also be spread perinatally from an untreated mother to her baby to produce neonatorum or pneumonia in some exposed infants. Despite aggressive control programs, rates of *C. trachomatis* infection have continued to increase. Novel strategies to prevent and treat *C. trachomatis* infection effectively are needed.

C. trachomatis undergoes a unique developmental cycle that begins with the attachment of infectious elementary bodies (EBs) to eukaryotic host cells (Moulder 1991; Abdelrahman and Belland 2005). After EBs enter into cells, they reside in a membrane-bound inclusion and differentiate into non-infectious, replicating reticulate bodies (RBs). RBs then asynchronously re-differentiate into EBs prior to release from host cells. These released EBs are infectious and can invade neighboring cells, exacerbating infection. *C. trachomatis* infection of epithelial cells evokes an increased synthesis and secretion of proinflammatory mediators, such as interleukin6 (IL6), IL1, tumor necrotic factor α (TNFα) and CXCL8 (Rasmussen, Echmann, Quayle, *et al.*, 1997; Buchholz and Stephens 2006). These mediators play an important role in the host immune response during infections and function to improve the clearance of pathogens. However, exacerbated inflammatory responses elicited by chronic infection or reinfection can lead to permanent tissue damage, tubal scaring and infertility (Gottlieb, Xu, Brunham, *et al.*, 2013; Darville and Hiltke 2010).

The treatments of chlamydial infection ideally eradicate persisting pathogens and prevent tissue damage. Azithromycin (a macrolide antibiotic) and doxycycline are the preferred antibiotics used to treat *C. trachomatis* infections. Recent studies highlight the value of these therapeutic drugs, macrolides in particular, as effective antimicrobial and anti-inflammatory agents in chronic bacterial infection and inflammation (Sweeney and Stamm. 2005; Srivastava, Ja, Vardhan, *et al.*, 2012; Altenburg, de Graaff, Stienstra, *et al.*, 2013). More recently, however, targeting virulence factors, such as the type III secretion system (T3SS) and quorum sensing (QS) or host-directed immunomodulatory therapies, represent novel strategies that would avoid potential antibiotic resistance in bacterial pathogens (Baron and Coombes 2007; Barczak and Hung 2009; Zigangirova, Zayakin, Kapotina, *et al.*, 2012; Rampioni, Lioni and Williams 2014). Efforts have also been made to identify natural components that may contribute to the treatment of various infectious diseases (Kalan and Wright 2011; Ma, Liu, Liang, *et al.*, 2012; Yilma, Singh, Morici, *et al.*, 2013). The herb *Andrographis paniculata* (Chuan Xin Lian) has been traditionally used to treat various diseases, including respiratory tract infection, in China and other Asian countries (Chao and Lin 2010; Jayakumar, Hsieh, Lee, *et al.*, 2013). In Chinese medicine theory, *A. paniculata* can cool down the internal heat caused by infection, reduce inflammation and stop pain. Its major derivative, Andrographolide (Andro), a labdane diterpene lactone product (Fig. 1a), has a wide range of bioactivity, including antibacterial, antiparasitic, antiviral, anticancer and antidiabetic properties, as reported in various laboratory studies (Wiart, Kumar, Yusof, *et al.*, 2005; Abu-Ghefreh, Canatan and Ezeamuzi 2009; Zheng, Liu and Guo 2012; Nugroho, Rais, Setiawan, 2014) and clinical trials (Calabrese, Berman, Babish, *et al.*, 2000; Coon and Ernst 2004; Jayakumar, Hsieh, Lee, *et al.*, 2013). Natural remedies such as Andro offer antimicrobial properties and may serve as an alternative or synergistic therapeutic to traditional antibiotics.

The aim of this study was to investigate the effect of Andro on *C. trachomatis* infection using a human cervical epithelial cell culture model. The time- and dose-dependent impacts of Andro on the *C. trachomatis* developmental cycle within host cells were established using strains LGV L2/434/Bu and the transformed strain L2GFP expressing green fluorescent protein (GFP). We have demonstrated that Andro exerts a dual role

in *Chlamydia*–host interaction: to perturb *C. trachomatis* transition from the metabolically active RB form to the infectious EB form and to reduce significantly the secretion of IL6, CXCL8 and interferon (IFN)-γ-induced protein10 (IP10) produced by epithelial cells following *C. trachomatis* infection. Future dissection of Andro's mode of action both against *Chlamydia* and as an anti-inflammatory agent may provide identification of novel therapeutic targets.

MATERIALS AND METHODS

Cell culture and reagents

A human cervical cancer cell line, HeLa 229 cells (CCL2, ATCC), and mouse fibroblast L929 cells (L cell, CCL-1, ATCC) were cultured in Dulbecco's modified Eagle's medium with high glucose (4.5 g/l) supplemented with 10% fetal bovine serum (Sigma-Aldrich) and L-glutamine (2 mM) at 37°C, in a humidified incubator with 5% CO_2. The medium excluded cycloheximide (a host cell protein synthesis inhibitor) to examine Andro's effects on both bacterial growth and the host immune response. Andrographolide ($C_{20}H_{30}O_5$, Andro, HPLC $\geq$98%), dimethylsulfoxide (DMSO) and ampicillin were purchased from Sigma-Aldrich. Andro stocks were dissolved in 100% DMSO at 30 mM. In all experiments, the Andro stock was diluted in the corresponding culture medium and controls were carried out using an equal percentage of DMSO.

C. trachomatis strains

The chlamydial shuttle plasmid pGFP::SW2 was kindly provided by Ian Clarke (University of Southampton, UK) (Wang, Kahane, Cutliffe, *et al*., 2011). *C. trachomatis* strains used in this study are: (i) wild-type L2/434/Bu containing a natural plasmid; and (ii) L2GFP that was generated by the transformation of pGFP::SW2 into a plasmid-less strain L2/25667R (kindly provided by Julius Schachter from the University of California at San Francisco) (Peterson, Markoff, Schacheter, *et al*., 1990) using the method described previously (Gong, Yang, Lei, *et al*., 2013). Single GFP-positive infected cells were isolated by plaque assay (Matsumoto, Miyashita and Ohuchi 1998) with ampicillin (5 μg/ml) selection. The clone of the *C. trachomatis* strain was amplified in an L929 suspension culture. EBs were purified by centrifugation on an OptiPrep density gradient medium as described previously (Frohlich, Hua, Wang, 2012), resuspended in cold sucrose-phosphate-glutamic acid (SPG) buffer (10 mM sodium phosphate [8 mM Na_2HPO_4, 2 mM NaH_2PO_4], 220 mM sucrose, 0.5 mM L-glutamic acid) and stored at −80°C until used. *C. trachomatis* stocks tested negative for mycoplasma by PCR (Ossewaarde, de Vries, Bestebroer, *et al*., 1996).

Cytotoxicity determination with Andro

A colorimetric cell counting kit-8 (CCK-8) (Biyuntian, Beijing, China) was used to determine the cytotoxic effect of Andro in HeLa 229 cells according to the manufacturer's instructions. Briefly, HeLa 229 cells were seeded at 5000 cells per well in 96-well plates and allowed to grow for 20 h. Monolayers with or without *C. trachomatis* infection were exposed to increasing concentrations of Andro (ranging from 0 to 220 μM) diluted in medium. Following a 44 h exposure to Andro, 10 μl of the cell counting reagent was directly added to the cultures. The plates were incubated for an additional 4 h at 37°C in a 5% CO_2 environment. The water-soluble formazan product was measured at 450 nm using a microplate reader (BioTek). Cytotoxicity was determined by comparing the resulting absorbance with the mean absorbance of the controls (with DMSO as 100% viability) and expressed as a percentage of cell viability.

C. trachomatis infection and Andro exposure

In the following experiments, monolayers of HeLa 229 cells in 96-well plates were inoculated with *C. trachomatis* EBs at a dose resulting in ∼40% of cells being infected, and centrifuged at 1600 *g* for 40 min at 37°C. Fresh medium was added to the infected cells and incubated at 37°C for various time periods as indicated in each experiment as below. (i) Andro response assay: various concentrations of Andro or DMSO were added to media immediately after infection. Infected cells were incubated at 37°C in a 5% CO_2 environment until 44 hours post-infection (h pi); (ii) Time of removal assay: *C. trachomatis*-infected cells were cultured in Andro-containing medium immediately after infection. The medium was then replaced with the DMSO-containing medium at 6 or 24 h pi. Cells were incubated up to 44 h pi before observation. (iii) Time of addition assay: Andro or DMSO was added to *C. trachomatis*-infected cell media at 0, 6 or 24 h pi and incubated at 37°C, 5% CO_2 until 44 h pi; (iv) Invasion inhibition assay: EBs (2×10^6) diluted in 1 ml of SPG were treated with 30 or 60 μM Andro or DMSO on ice for 1 h prior to infection. Next, HeLa 229 cells were inoculated with 10 μl of the EBs–Andro mixture (2×10^4 EBs) in each well. Infected cells were incubated at 37°C, 5% CO_2 for 44 h prior to observation. (v) Cell pre-treatment assay: HeLa 229 cells were cultured in Andro (30 or 60 μM) or DMSO-containing medium for 24 h prior to infection. Andro was removed from the culture with extensive washing and addition of Andro-free media. HeLa 229 cells were infected with EBs and cultured in Andro-free medium for 44 h before observation. To evaluate *C. trachomatis* infectivity, inclusions were enumerated by manual counting in triplicate wells. The results were converted to inclusion-forming units (IFUs) per 1 ml and then converted into percentages of *C. trachomatis* infectivity relative to the DMSO controls.

Endpoint IFU assay

C. trachomatis-infected cells were harvested in SPG at the time points indicated in each assay and subcultured by infecting HeLa 229 cell monolayers with serial dilutions. The quantity of infectious progeny was determined by IFU enumeration from triplicate wells using fluorescence microscopy. The total numbers were presented as IFUs/ml in each result.

Antibodies

The primary antibodies used to detect chlamydial antigens were rabbit polyclonal antibodies against inclusion membrane protein IncA (kind gift from Ted Hackstadt, Rocky Mountain Laboratories), cysteine-rich protein OmcB (kind gift from Tom Hatch, University of Tennessee) and a mouse monoclonal antibody specific to the MOMP of LGV serovar L2 (L2-14) (kind gift from Youxun Zhang, Boston University).

Indirect immunofluorescence assays

C. trachomatis-infected cells were grown on 12 mm diameter glass coverslips in 24-well plates and fixed at the time indicated in each result. The 2% paraformaldehyde-fixed and 4% saponin-permeabilized cells were incubated with primary

antibodies overnight at 4°C, followed by either Alexa 568- (red) or fluorescein isothiocyanate (FITC; green)-conjugated secondary antibodies (Molecular Probes) for 45 min at 37°C. Cells were counterstained with 4′,6-diamidino-2-phenylindole dihydrochloride (DAPI). Cells were visualized using an inverted fluorescent microscope (Zeiss Axio Observer D1). Images were taken and processed using AxioVision software version 4.8.

Multiplexed cytometric bead array assay

HeLa 229 cells infected with *C. trachomatis* (>90% infection rate) were grown in 96-well plates in the presence or absence of Andro. Cell-free culture supernatants were collected at 18 and 42 h pi, respectively. A panel of seven proinflammatory cytokines and chemokines, comprising IL1α, IL1β, TNFα, IL6, CXCL8, monocyte chemoattractant protein 1 (MCP1) and IP10, were simultaneously quantified using a multiplexed cytometric bead array assay (Millipore) according to the manufacturer's instructions. In control experiments, culture supernatant from mock-infected HeLa 229 cells were used.

Electron microscopy

C. trachomatis-infected cells were trypsinized, pelleted by a brief centrifugation (200 g for 2 min), fixed with 2% paraformaldehyde and 2.5% glutaraldehyde (Polysciences Inc., Warrington, PA, USA) in 200 mM phosphate buffer and processed as described previously (Beatty 2006). Ultrathin sections were cut with a Leica Ultracut UCT ultramicrotome (Leica Microsystems Inc., Bannockburn, IL, USA). Samples were viewed on a JEOL 1200 EX II transmission electron microscope (JEOL USA Inc., Peabody, MA, USA) equipped with an AMT 8 megapixel digital camera (Advanced Microscopy Techniques, Woburn, MA, USA).

Statistical analyses

Statistical analyses were performed using GraphPad PRISM software package. Non-linear regression analysis was performed to determine the 50% cytotoxic concentration (CC$_{50}$) of HeLa 229 cells or 50% inhibitory concentrations (IC$_{50}$s) of *C. trachomatis* infection in HeLa 229 cells. One-way analysis of variance (ANOVA) with a Bonferroni post-test was used for differences between Andro-exposed and non-exposed groups. Values of *P < 0.05, **P < 0.01 and ***P < 0.001 were considered statistically significant.

RESULTS AND DISCUSSION

Determination of Andro cytotoxicity with HeLa 229 cells

Andro is classified as a labdane diterpene lactone and, as such, is able to cross eukaryotic cell membranes (Fig. 1a). We sought to determine the possible cytotoxic effects of Andro using our model cervical cell line, HeLa 229 cells, to establish a range of Andro concentrations with minimal cytotoxic effect. CCK-8 assays were used to evaluate Andro's effect on dehydrogenase activity, an indicator of cell viability, in the presence of Andro or DMSO for 44 h. Minimal cytotoxicity associated with the exposure of cells to Andro within the concentration ranging from 0 to 60 μM was detected. When ≤60 μM Andro was used, there was >90% cell viability in Andro-exposed samples compared with DMSO-exposed controls. To establish a CC$_{50}$ of Andro for HeLa 229 cells, the amounts of Andro were increased to 220 μM (Fig. 1b). The percentage cell viability was examined and the mean CC$_{50}$ ± standard error of mean (SEM) was determined to be

125.2 ± 3.937 μM for *C. trachomatis* L2GFP-infected cells, versus 131.3 ± 2.584 μM for uninfected cells by non-linear regression analysis. There was no significant difference in cell viability between the *C. trachomatis*-infected and uninfected cells (P > 0.05). Considering the large effect on cell viability that was observed at Andro amounts >100 μM (<80% cell viability), further experiments determining the effect of Andro on *C. trachomatis* were conducted using concentrations of Andro ≤60 μM.

Andro exposure inhibits *C. trachomatis* inclusion formation and reduces infectious progeny yields

The potency of Andro on *C. trachomatis* infection has not been investigated. To this end, we performed a dose–response experiment with increasing Andro concentrations. The *C. trachomatis* inclusions were quantitated and the results were converted to percentage infectivity compared with DMSO-exposed control. Figure 2a and b shows that both L2/434 and the transformed L2GFP strains were susceptible to Andro in a dose-dependent manner during the 44 h observation period *in vitro*. In addition to the lower infectivity, there were smaller inclusions in Andro-exposed samples than in DMSO-exposed controls. Using non-linear regression analysis, the IC$_{50}$s of Andro for *C. trachomatis*-infected HeLa 229 cells were determined to be 46.54 ± 1.174 μM (mean ± SEM) against L2/434-infected cells and 50.62.17 ± 2.157 μM against L2GFP-infected cells. Within the range of IC$_{50}$s, no significant change in host cellular morphology was observed (data not shown). Cell viability, as measured by CCK-8 assay, was not significantly different from the DMSO control (Fig. 1b). These results suggest that the observed inhibitory effect of Andro on *C. trachomatis* is not a result of cellular toxicity.

A critical step in chlamydial development is the RB to EB transition. This transition can often be blocked in the presence of subinhibitory concentrations of antibiotics or under nutrient depletion in the cultures (Beatty, Belanger, Desai, *et al*., 1994; Harper *et al*., 2000; Wyrick 2010). To address whether Andro represses the production of progeny EB, IFU assays were performed using infected cells and culture supernatants; both were sampled at 36 h pi prior to cell lysis by infection. At this time, the culture supernatant may contain progeny EBs released from cells through mechanisms of extrusion (Hybiske and Stephens 2007). In the presence of 30 or 60 μM Andro, a significant decline in L2/434 IFUs and L2GFP IFUs was observed using infected cells (Fig. 2c). Similarly, IFUs in the culture supernatants dropped as compared with the unexposed control for both L2/434 and L2GFP (Fig. 2d), suggesting that a premature release of EBs is unlikely to be the major reason for the decreased EB yields induced by Andro. These data suggest that Andro inhibits the chlamydial infection by disrupting the RB to EB transition. Thus, the decrease in IFUs is a direct indication of Andro's effects on *C. trachomatis* growth.

Rapidly dividing chlamydial organisms are susceptible to Andro exposure *in vitro*

In order to determine the point at which the chlamydial developmental cycle was affected by Andro, we conducted a series of assays with *C. trachomatis* L2GFP by examining the changes in IFUs induced by Andro. Under our experimental conditions, the developmental cycle for both *C. trachomatis* L2GFP and L2/434 took ~48 h to complete. Pre-exposure of EBs to Andro at a concentration of 30 or 60 μM did not significantly decrease IFUs compared with unexposed EBs, suggesting that Andro did not directly impede EB invasion (data not shown). We next pre-exposed HeLa
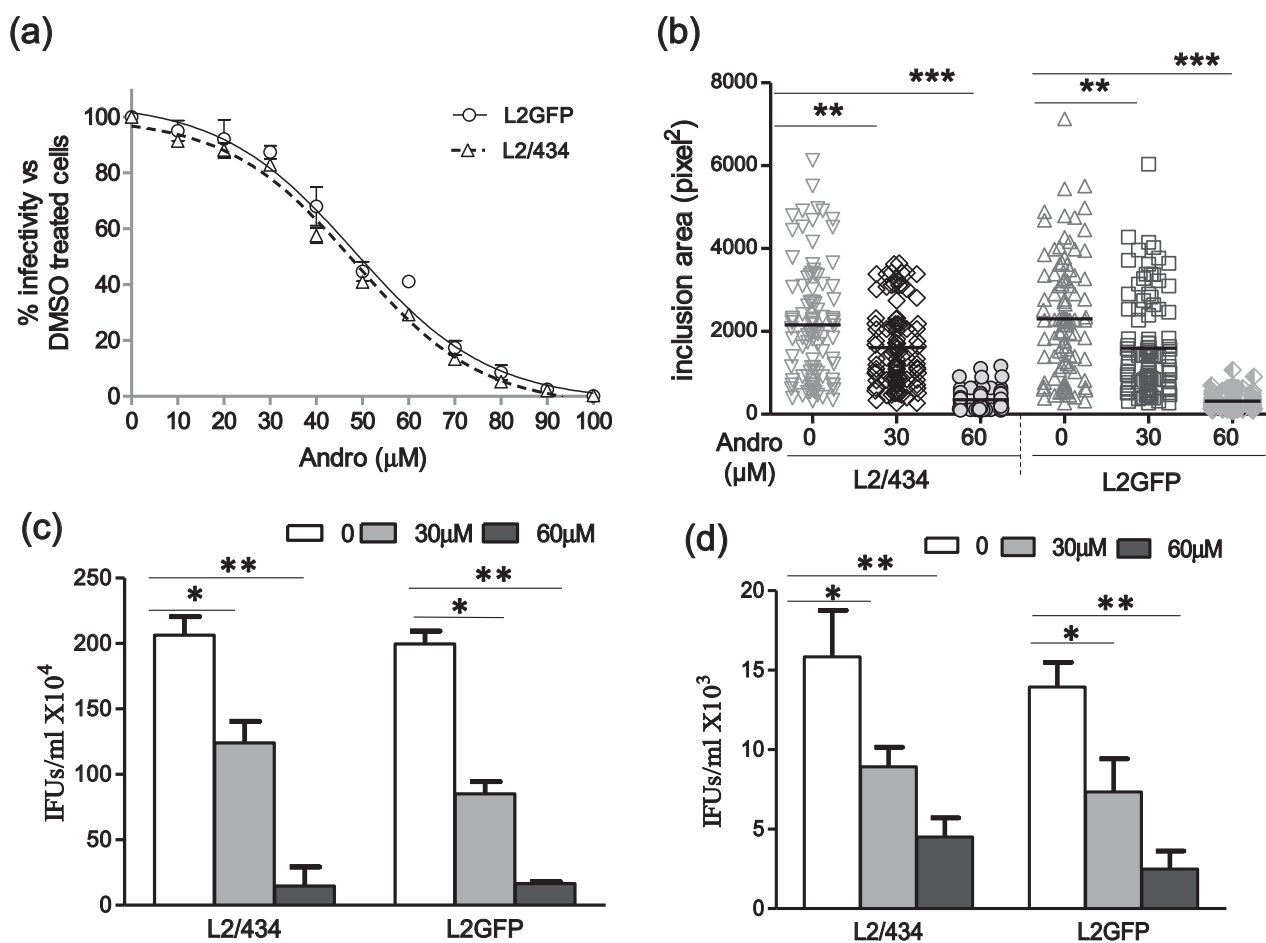
Figure 2. Inhibitory effect of Andro on *C. trachomatis* growth. (**a**) Dose–response curves for *C. trachomatis*-infected HeLa 229 cells exposed to Andro. Cells infected with *C. trachomatis* L2/434 (△) or L2GFP (○) were fixed at 44 h pi and processed for IFA. The data represent the mean ± SEM from three separate experiments, in which quadruplicates were tested. (**b**) Changes in inclusion sizes induced by Andro. Infected cells were exposed to Andro at increasing concentrations of 0, 30 and 60 μM. One hundred inclusions were measured for each category from three separate experiments. The area data represent the mean ± SEM. The *P*-value was determined using one-way ANOVA with a Bonferroni test. (**c**) Determination of EB progeny yields by IFU assays with *C. trachomatis*-infected HeLa 229 cells. (**d**) Determinination of EB progeny yields by IFU assays with culture supernatants. Samples were collected at 36 h pi. Shown are representative results from three separate experiments, in which triplicates were tested. Data bars represent the mean ± standard deviation (SD). The *P*-value was determined using one-way ANOVA with a Bonferroni test. *$P < 0.05$, **$P < 0.01$ and **$P < 0.001$.

229 cells to Andro at a concentration of 30 or 60 μM for 24 h prior to infection. The resultant chlamydial IFUs were similar to those observed in unexposed HeLa 229 cells, suggesting that Andro was unable to prevent *C. trachomatis* from entry through modulating host cell factors under our test conditions (data not shown). Based on the finding that Andro at a concentration of 30 μM was sufficient to reduce EB production (Fig. 2), we conducted time of addition/removal assays with 30 μM Andro. Addition of Andro to *C. trachomatis*-infected cells at 0 or 6 h pi, but not at 24 h pi, caused a significant decrease in IFUs in samples collected at 44 h pi (Fig. 3a and b), suggesting the stage-specific effect of Andro. This observation was further confirmed by a time of removal assay (Fig. 3c and d). Removal of Andro from *C. trachomatis* cultures exposed to Andro for a 6 or 24 h period resulted in significantly fewer IFUs than in unexposed infected cells collected at 44 h pi. However, a short exposure (6 h) was less effective. Overall, these results indicate that Andro inhibits *C. trachomatis* infection of HeLa 229 cells in an entry-independent and growth stage-dependent manner, with the optimal inhibitory effect of Andro occurring prior to 24 h pi during RB growth and division.

Andro exposure reduces levels of late stage expressed OmcB protein

Chlamydia spp. growth occurs exclusively in the inclusion. There were significantly irregular inclusions induced by 60 μM Andro. Therefore, we examined Andro's impact on inclusion membrane protein localization and EB maturation in *C. trachomatis* L2GFP-infected cells in the presence of 30 μM Andro using indirect fluorescence assays (IFAs). First, we examined IncA protein that is normally expressed at the mid-stage of growth and is then secreted to the inclusion membrane through the T3SS, all of which is required for homotypic inclusion fusion (Rockey, Grosenbach, Hruby, *et al.*, 1997). Secondly, we examined the cysteine-rich OmcB protein that is a key component of the disulfide-cross-linked envelope protein complex found in EBs (Hackstadt and Caldwell 1985; Hatch 1996). Despite the smaller size of chlamydial inclusions induced by Andro, most of the inclusions remained intact, and localization of IncA (red) in the inclusion membrane was observed (Fig. 4a). This latter finding reflects the ability of chlamydial organisms to synthesize and secrete IncA in the presence of a low dose of Andro, a
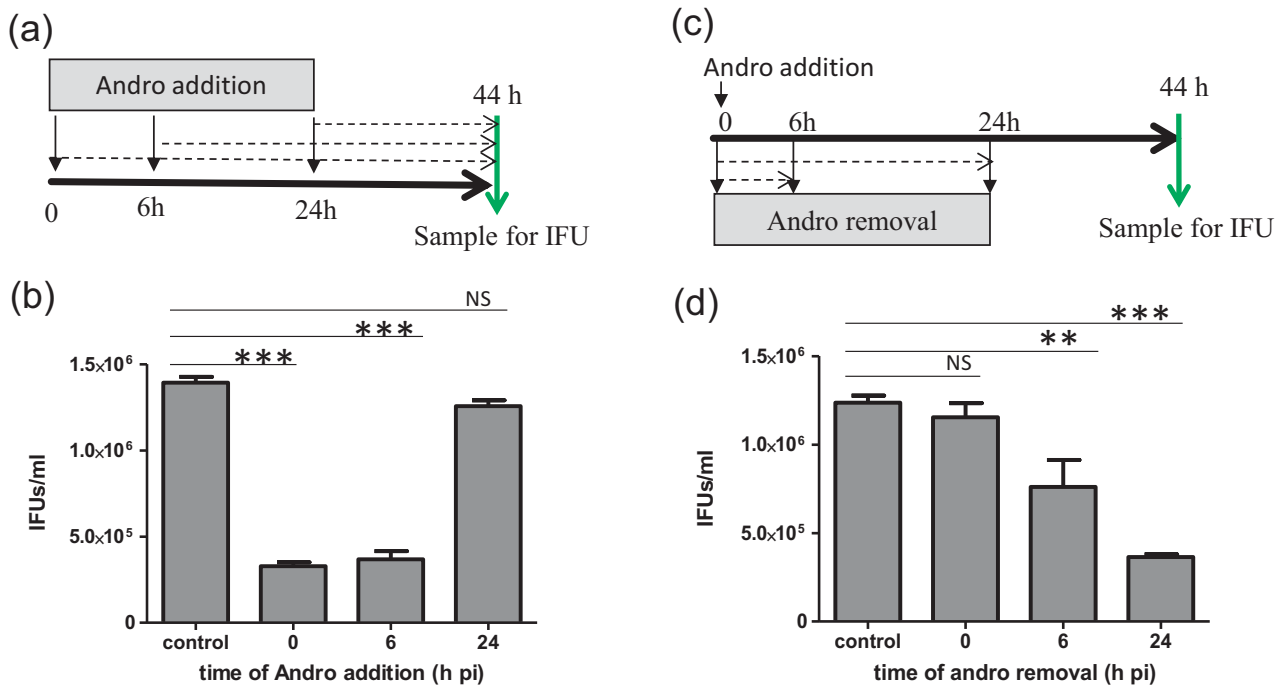
Figure 3. Time-dependent effect of Andro on *C. trachomatis* growth. (**a**) Experimental schematic for the time of addition assay. *C. trachomatis* L2GFP-infected cells were exposed to Andro (30 μM) at 0, 6 or 24 h pi and culture was continued until 44 h pi for IFU assay. (**b**) IFU assessment for a time of addition assay. (**c**) Experimental schematic for the time of removal assay. *C. trachomatis* L2GFP-infected cells were exposed to Andro (30 μM) immediately after infection for a period of 0, 6 or 24 h pi. The medium was then replaced with the DMSO-containing medium. Cells were examined at 44 h pi for IFU assay. (**d**) IFU assessment for a time of removal assay. IFU values are reported as the mean $\pm$ SD. Results indicate mean IFU values $\pm$ SD in triplicate. Cells cultured in DMSO-containing medium were used as controls. The P-value was determined using one-way ANOVA with a Bonferroni test. **$P < 0.01$, ***$P < 0.001$, NS, non-significant.

process which can be disrupted by T3SS inhibitors or conditions of iron deprivation (Wolf, Betts, Chellas-Gery, *et al*., 2006; Zigangirova, Zayakin, Kaptina, *et al*., 2012). During the late stage of *C. trachomatis* growth, we observed, in unexposed cells, abundant small, scattered EBs that expressed OmcB (red) within inclusions (Fig. 4b, upper panel). In contrast, at the same time point, there was much less OmcB observed in Andro-exposed inclusions (Fig. 4b, lower panel). This observation supports our IFU findings (Fig. 2c and d) and verifies that fewer OmcB-expressing EBs were produced upon exposure to Andro. Given the importance of OmcB in the structural stability of EBs, it is likely that an altered chlamydial form is induced by Andro.

Andro exposure induces structural alternations in chlamydial organisms

To test this possibility, we analyzed the ultrastructure of chlamydial organisms exposed to 30 μM Andro by transmission electron microscopy (TEM). Cross-sections revealed that, unlike the unexposed cells (Fig. 5a, d and e), Andro exposure induced inclusions containing fewer chlamydial particles, including intermediate body (IB)-, RB- and EB-like forms during the 36 h observation period (Fig. 5b and f). Strikingly, high magnification images clearly revealed that only Andro-exposed cells displayed deformed chlamydial organisms with irregular membranes and blebbing-like material on their surface (Fig. 5c and g). There also appeared to be numerous small membrane vesicles (MVs) and low electron-dense precipitations in the inclusion lumen. These observations were unusual but unlikely to have been an artifact of TEM processing since unexposed control cells exhibited little to no evidence of such phenotypes (Fig. 5a, d and e). It

was unclear whether these deformed *C. trachomatis* forms were stably present or eventually underwent cell lysis. Nevertheless, these TEM studies in combination with the decrease in OmcB expression (Fig. 4) as well as decreased IFUs (Fig. 3) provide further evidence for a perturbation of *C. trachomatis* growth and EB production induced by Andro.

Morphological abnormalities of chlamydial organisms have often been associated with a persistent growth state of *C. trachomatis in vitro* under adverse growth conditions. For example, aberrant enlarged RBs can be induced by nutrient (amino acid, glucose and iron) deprivation (Harper, Pogson, Jones, *et al*., 2000; Slepenkin Enquist, Hagglund, *et al*., 2007; Gussmann, Al-Younes, Braun, *et al*., 2008), IFN-γ exposure that diminishes the pool of tryptophan by inducing indoleamine 2,3-dioxygenase (IDO) in host cells (Beatty, Belanger, Desai, *et al*., 1994) or in the presence of subinhibitory concentration of antibiotics (Engel 1992; Wyrick 2010). Additionally, it was shown that irregular *C. trachomatis* forms were induced by LpxC inhibitors that blocked the biosynthesis of lipid A in *C. trachomatis* (Nguyen, Cunningham, Liang, *et al*., 2011). Unlike the morphological changes described above, Andro induces a subtle, but distinct structural consequence that is typified by the damaged chlamydial membranes. We also observed an accumulation of MVs. It is noteworthy that *Chlamydia* spp. naturally produce MVs during replication (Stirling and Richmond 1980) and excess MVs were produced under stress conditions (for a review, see Frohlich, Hau, Quayle, *et al*., 2014). The present study cannot distinguish whether increased MV formation is the result of an Andro-triggered specific bacterial responses and/or a general stress response. Adding excess tryptophan or glucose to the culture media failed to reverse the Andro-induced chlamydial impairment (our unpublished data), suggesting that neither
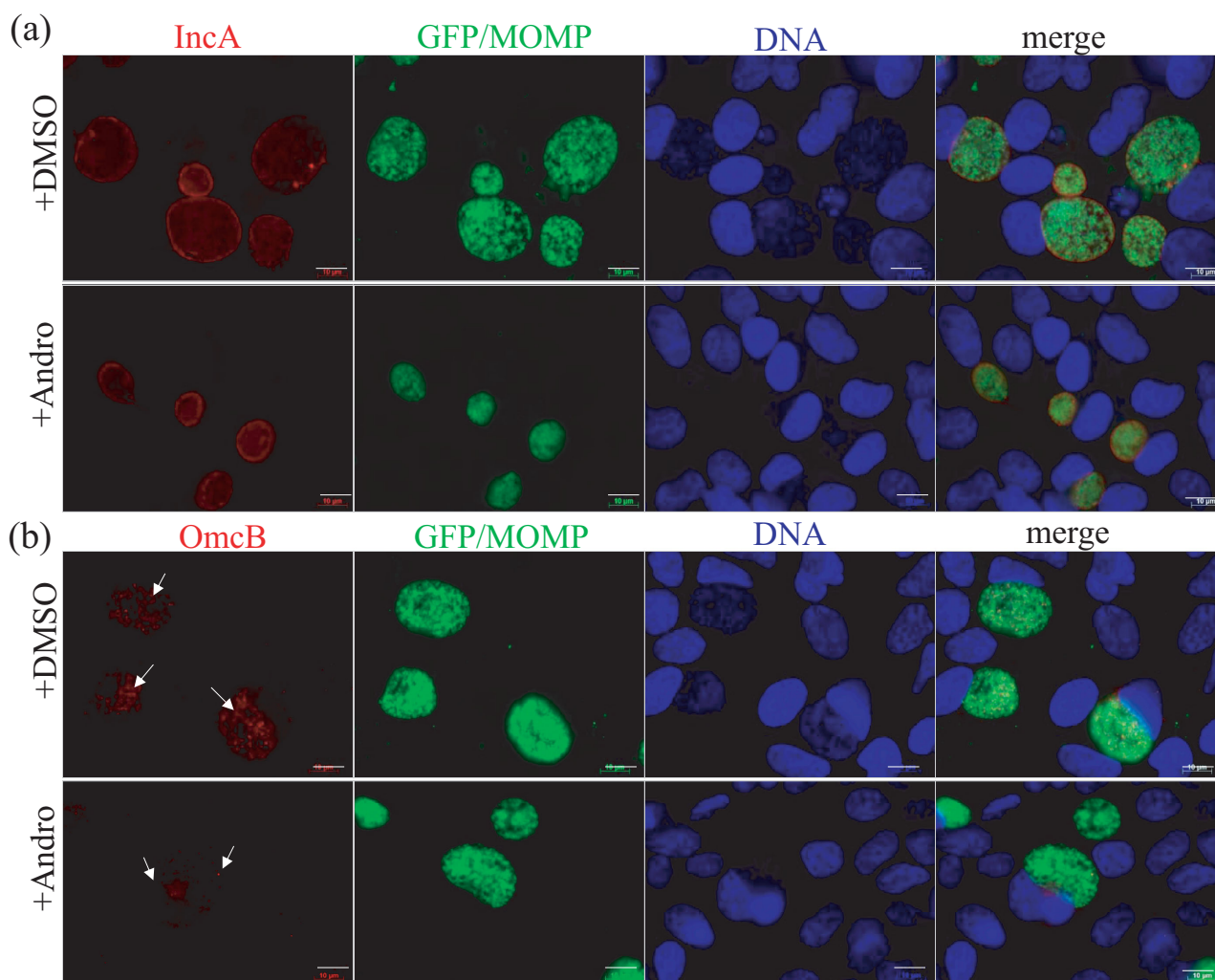
Figure 4. Visualization of chlamydial IncA and OmcB expression by IFA in the presence or absence of Andro. (**a**) Representative *C. trachomatis*-infected cells co-stained with IncA (red) and GFP/MOMP (green). (**b**) Representative *C. trachomatis*-infected cells co-stained with OmcB (red) and GFP/MOMP (green). HeLa 229 cells infected with *C. trachomatis* L2GFP exposed to Andro (30 μM) for 44 h were fixed and processed for IFA. The IncA and OmcB proteins (red) were probed with polyclonal antibodies against IncA and OmcB, respectively. Chlamydial organisms were visualized by GFP and MOMP staining with anti-MOMP antibody (green). DNA was counterstained with DAPI (blue). Images were obtained under the same exposure conditions. Note: more abundant, scattered, OmcB-expressing EBs were identified in unexposed cells, but not in Andro-exposed cells as indicated by arrows. Scale bar = 10 μm.

tryptophan nor glucose depletion is the mechanism of Andro's anti-*Chlamydia* action.

The use of Andro or its analogs has been shown to weaken virulence and biofilm formation in various bacteria, including drug-resistant *Staphylococcus aureus* and *Pseudomonas aeruginosa* (Zaidan, Noor Rain, Badrul, *et al.*, 2005; Ma, Liu, Liang, *et al.*, 2012). Interestingly, Andro's impact is not due to the direct elimination of viable bacteria, but rather the suppression of the synthesis of toxins and QS signal molecules, known as autoinducers (AIs) that include AI2 and *N*-acylhomoserine lactones (AHLs). QS permits bacterial cell–cell communication and co-ordination of virulence gene expression as a result of discerning AIs. Neither functional QS nor the signals that co-ordinate *C. trachomatis* virulence at the population level has been documented. Recently, the importance of the methyl cycle has begun to be appreciated in *C. trachomatis* (Binet, Fernandez, Fisher, *et al.*, 2011). In bacteria, the methyl cycle recycles adenine and methionine via S-adenosylmethionine (SAM)-mediated methylation and produces AI-2. SAM is also essential for the synthesis of AHLs. Despite the lack of a *metK* homolog,

needed for SAM synthesis, *C. trachomatis* possesses CTL843 that encodes a SAM/adenosylhomocysteine (SAH) transporter. This transporter allows *C. trachomatis* to acquire SAM from the host cell and excrete the toxic by-product SAH (Binet, Fernandez, Fisher, *et al.*, 2011). Whether Andro, at the minimum cellular toxicity concentration, might mimic signal molecules, modulating specific bacterial pathways, such as methylation, remains to be determined.

Andro significantly represses cytokine secretion by *C. trachomatis*-infected epithelial cells

To examine Andro's effect on the innate immune response to chlamydial infection, we measured secretion of a panel of seven cytokines and chemokines from *C. trachomatis*-infected cultures. As expected, there was a significant increase in levels of the proinflammatory cytokine IL6, and the chemokines CXCL8 and IP10 by >4-fold following infection with either *C. trachomatis* L2/434 or L2GFP compared with mock-infected cells (Fig. 6).
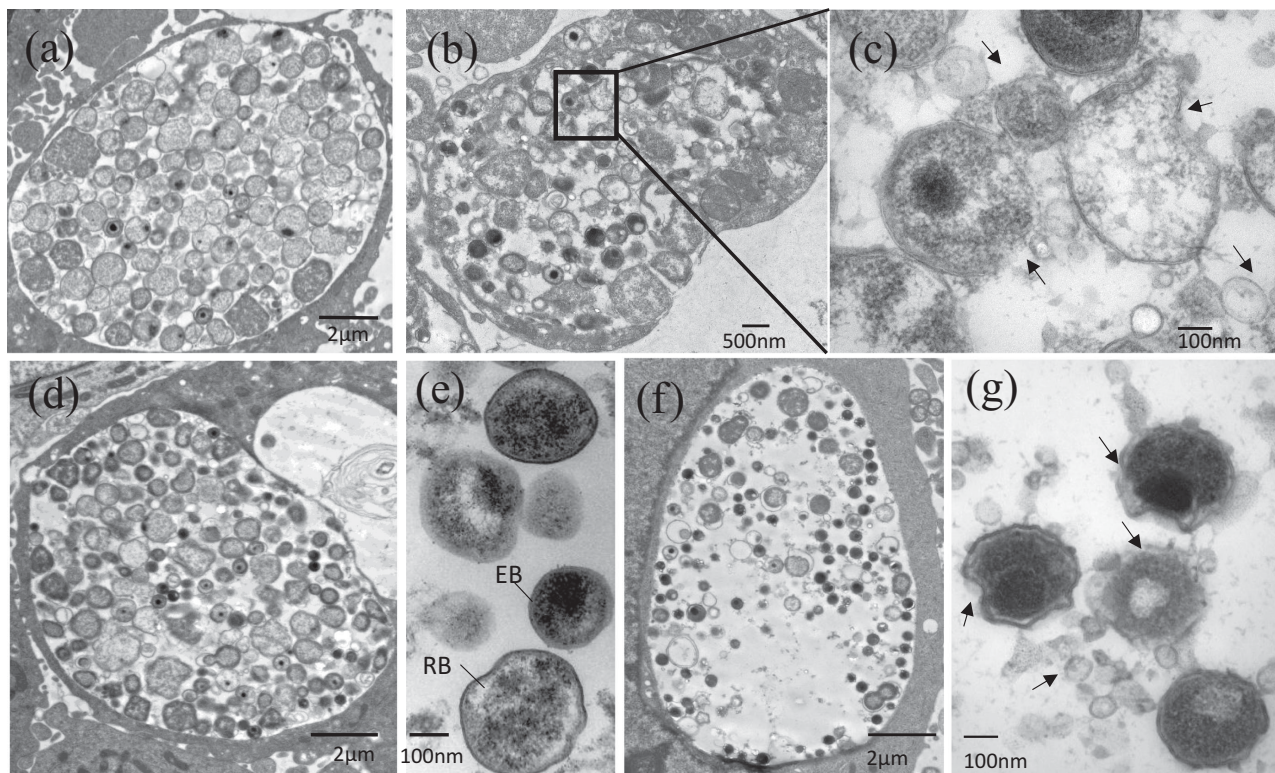
Figure 5. Altered ultrastructure of chlamydial organisms in HeLa 229 cells induced by Andro. (**a–c**) Representative micrographs of infected cells fixed at 28 h pi. Cells unexposed (a) or exposed (b and c) to Andro (30 μM). An enlarged image from the box in (b) is shown in (c). (**d–g**) Representative micrographs of infected cells fixed at 36 h pi. Cells unexposed (d and e) or exposed (f and g) to Andro (30 μM). Note: deformed chlamydial organisms were only observed in *C. trachomatis*-infected cells exposed to Andro as indicated in (b), (c), (f) and (g). Arrows indicate irregular *C. trachomatis* membranes and MV accumulation induced by Andro. Scale bar for (a), (d) and (f) = 2 μm, for (b) = 500 μm, and for (c), (e) and (g) = 100 nm.

There was a modest (~2.5-fold), yet statistically insignificant elevation of TNFα induced by L2/434 and L2GFP infection relative to the control. No significant difference in secretion of IL1α, IL1β and MCP1 was observed between L2/434- or L2GFP-infected cells and the mock-infected controls (data not shown). This may reflect insufficient accumulation or release of these cytokines prior to cell lysis (42 h pi). This is in agreement with previous reports demonstrating that IL1 is released $\geq$48 h pi after cell lysis by infection (Rasmussen, Eckmann, Quayle, *et al.*, 1997; Buckner, Lewis, Greene, *et al.*, 2013). High levels of IL6, CXCL8 and IP10 were found at 42 h pi, but not at 18 h pi (Fig. 6), indicating a delayed cytokine response to *C. trachomatis* infection that is consistent with previous observations (Rasmussen, Eckmann, Quayle, *et al.*, 1997; Buchholz and Stephens 2006; Buckner, Lewis, Greene, *et al.*, 2013). In contrast, Andro exposure resulted in significantly decreased secretion of IL6, CXCL8 and IP10, by >3.6-fold in both L2/434- and L2GFP-infected cultures as determined at 42 h pi (Fig. 6). Andro itself had no significant effect on mock-infected cells. Moreover, the levels of IL1α, IL1β, TNFα and MCP1 remained constant at low levels. These data indicate that Andro represses the host signaling pathways relevant to IL6, CXCL8 and IP10 production in addition to its growth inhibition effect on *C. trachomatis*.

The finding that L2/434 and L2GFP infections elicit similar cytokine profiles suggests that the presence of the shuttle plasmid and expression of GFP do not impair the ability of *C. trachomatis* to stimulate a host immune response in HeLa 229 cells. The production of cytokines that have chemoattractant and proinflammatory functions, such as CXCL8, IL6 and IP10, is a critical immune response to *C. trachomatis* infection. However, cytokine constitutive expression or overproduction may have deleterious effects involving chronic chlamydial infections (Rasmussen, Eckmann, Quayle, *et al.*, 1997; Herrera, Shen, Lopez, *et al.*, 2003; Buchholz and Stephens 2006; Darville and Hiltke 2010). The Andro-induced decline in cytokine secretion by *C. trachomatis*-infected cells may reflect limited stimulation due to fewer chlamydial organisms or an altered chlamydial protein profile. In addition, Andro was shown to directly modulate host signaling pathways, such as nuclear factor-κB (NF-κB) (Abu-Ghefreh, Canatan, Ezeamuzie, *et al.*, 2009; Chao, Kuo, Lin, *et al.*, 2011; Hsieh, Hsu, Hsiao, *et al.*, 2011; Lee, Chang, Chung, *et al.*, 2011). The exact mechanism by which *C. trachomatis* stimulates the innate response remains incompletely known, but appears to require activation of complex signal transduction cascades, including NF-κB and mitogen-activated protein kinase (MAPK) pathways in both epithelial cells and macrophages (Buchholz and Stephens 2006; Zhou, Huang, Li, *et al.*, 2013). Given that many proinflammatory cytokines, including CXCL8, IL6 and IP10, are regulated by NF-κB, Andro modulation of NF-κB pathways may be one explanation for a decreased proinflammatory innate response in epithelial cells. Several questions arise from our studies and include the following. How does Andro modulate the host cytokine response to *C. trachomatis* infection? What role does Andro-induced downregulation of IL6, CXCL-8 and IP10 play in the context of chlamydial clearance *in vivo*? We are currently addressing these and other questions in an effort to understand further *C. trachomatis* pathogenesis in the context of host–pathogen interaction.
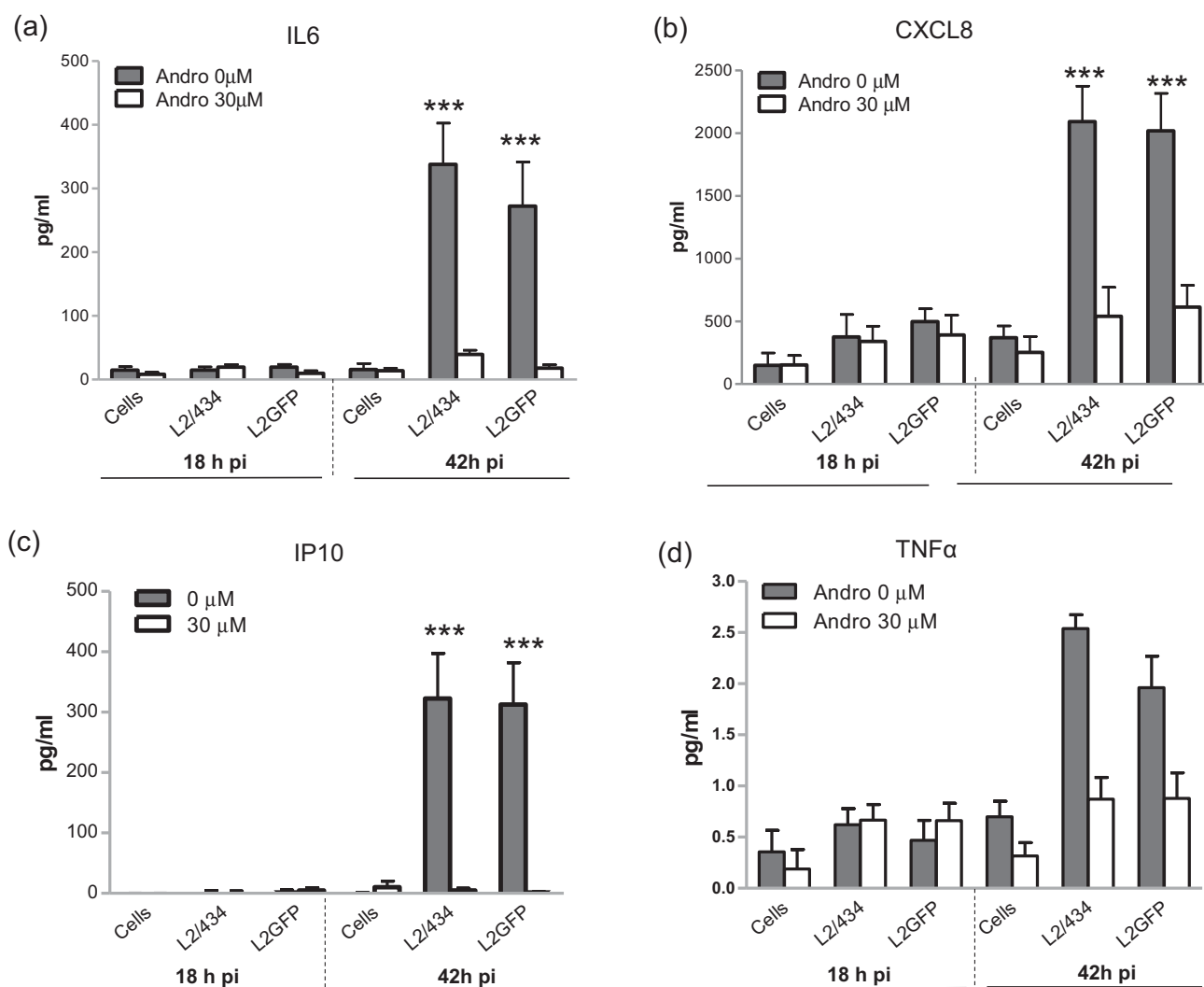
Figure 6. Suppression of proinflammatory cytokine secretion from *C. trachomatis*-infected epithelial cells by Andro. (**a**) IL6; (**b**) CXCL8; (**c**) IP10; (**d**) TNFα. HeLa 229 cells were infected with EBs of L2/434 or L2GFP, followed by the immediate addition of Andro (30 μM) to the culture. Culture supernatants were collected at 18 and 42 h pi and measured for levels of cytokines using cytometric bead assays. Data bars show the mean $\pm$ SD (pg/ml). ***P $<$ 0.001, compared with the mock-infected cell control using one-way ANOVA and Bonferroni's test. No significant difference in TNFα production was observed between L2/434- or L2GFP-infected cells and the mock-infected control (P $>$ 0.05).

Andro is commercially available for oral administration or injection. Its topical utilization may be limited due to low solubility, but, given the potent antimicrobial activity of this natural component, promising rational designs to synthesize new derivatives with increased solubility while retaining antimicrobial activity for treatment of infectious diseases have emerged. Several *in vivo* studies on the efficacy of Andro against microbes with few side effects have been completed. Reasonably strong evidence from clinical trials suggests that Andro is effective in reducing the severity and the duration of upper respiratory tract infection when treatment is started within the first 36–48 h of symptoms (Coon and Ernst 2004; Jayakumar, Hsieh, Lee, *et al.*, 2013). Another study (Calabrese, Berman, Babish, *et al.*, 2000) demonstrated a significant rise in the CD4^{+} lymphocyte level of HIV-positive subjects after Andro administration. Furthermore, it was found that treatment with Andro's analogs significantly suppressed inflammation in a rat endometriosis model (Zheng, Liu, Guo, *et al.*, 2012). There are no safe vaccines and only

limited antibiotics available to prevent or treat chronic *C. trachomatis* infections. Andro and its derivatives may be useful for mitigating *C. trachomatis*-related inflammation as adjunct treatments to work synergistically with existing antibiotics (Kalan and Wright 2011). It is plausible that Andro may exert its antibacterial and anti-inflammatory activity by targeting both bacterial factors and host signaling pathways. Further dissection of Andro's mode of action is warranted in order to pursue Andro and its analogs as a potential novel therapeutic reagent against *C. trachomatis* diseases.

ACKNOWLEDGEMENTS

REFERENCES

Abdelrahman YM, Belland RJ. The chlamydial developmental cycle. *FEMS Microbiol Rev* 2005;**29**:949–59.

Abu-Ghefreh AA, Canatan H, Ezeamuzie CI. *In vitro* and *in vivo* anti-inflammatory effects of andrographolide. *Int Immunopharmacol* 2009;**9**:313–8.

Altenburg J, de Graaff CS, Stienstra Y, *et al*. Effect of azithromycin maintenance treatment on infectious exacerbations among patients with non-cystic fibrosis bronchiectasis: the BAT randomized controlled trial. *JAMA* 2013;**309**:1251–59.

Barczak AK, Hung DT. Productive steps toward an antimicrobial targeting virulence. *Curr Opin Microbiol* 2009;**12**:490–96.

Baron C, Coombes B. Targeting bacterial secretion systems: benefits of disarmament in the microcosm. *Infect Disord Drug Targets* 2007;**7**:19–27.

Beatty WL. Trafficking from CD63-positive late endocytic multivesicular bodies is essential for intracellular development of *Chlamydia trachomatis*. *J Cell Sci* 2006;**119**:350–59.

Beatty WL, Belanger TA, Desai AA, *et al*. Tryptophan depletion as a mechanism of gamma interferon-mediated chlamydial persistence. *Infect Immun* 1994;**62**:3705–11.

Beatty WL, Belanger TA, Desai AA, *et al*. Role of tryptophan in gamma interferon-mediated chlamydial persistence. *Ann NY Acad Sci* 1994;**730**:304–6.

Binet R, Fernandez RE, Fisher DJ, *et al*. Identification and characterization of the *Chlamydia trachomatis* L2 S-adenosylmethionine transporter. *MBio* 2011;**2**:e00051–00011.

Buchholz KR, Stephens RS. Activation of the host cell proinflammatory interleukin-8 response by *Chlamydia trachomatis*. *Cell Microbiol* 2006;**8**:1768–79.

Buckner LR, Lewis ME, Greene SJ, *et al*. *Chlamydia trachomatis* infection results in a modest pro-inflammatory cytokine response and a decrease in T cell chemokine secretion in human polarized endocervical epithelial cells. *Cytokine* 2013;**63**:151–65.

Calabrese C, Berman SH, Babish JG, *et al*. A phase I trial of andrographolide in HIV positive patients and normal volunteers. *Phytother Res* 2000;**14**:333–8.

Chao WW, Lin BF. Isolation and identification of bioactive compounds in Andrographis paniculata (Chuanxinlian). *Chin Med* 2010;**5**:17.

Chao WW, Kuo YH, Lin BF. Anti-inflammatory activity of new compounds from Andrographis paniculata by NF-kappaB transactivation inhibition. *J Agric Food Chem* 2011;**58**:2505–12.

Cohen CR, Koochesfahani KM, Meier AS, *et al*. Immunoepidemiologic profile of *Chlamydia trachomatis* infection: importance of heat-shock protein 60 and interferon- gamma. *J Infect Dis* 2005;**192**:591–9.

Coon JT, Ernst E. Andrographis paniculata in the treatment of upper respiratory tract infections: a systematic review of safety and efficacy. *Planta Med* 2004;**70**:293–98.

Darville T, Hiltke TJ. Pathogenesis of genital tract disease due to *Chlamydia trachomatis*. *J Infect Dis* 2010;S114–125.

Engel JN. Azithromycin-induced block of elementary body formation in *Chlamydia trachomatis*. *Antimicrob Agents Chemother* 1992;**36**:2304–9.

Frohlich K, Hua Z, Quayle AJ, *et al*. Membrane vesicle production by *Chlamydia trachomatis* as an adaptive response. *Front Cell Infect Microbiol* 2014;**4**.

Frohlich K, Hua Z, Wang J, *et al*. Isolation of *Chlamydia trachomatis* and membrane vesicles derived from host and bacteria. *J Microbiol Methods* 2012;**91**:222–30.

Gong S, Yang Z, Lei L, *et al*. Characterization of *Chlamydia trachomatis* plasmid-encoded open reading frames. *J Bacteriol* 2013;**195**:3819–26.

Gottlieb SL, Brunham RC, Byrne GI, *et al*. Introduction: the natural history and immunobiology of *Chlamydia trachomatis* genital infection and implications for chlamydia control. *J Infect Dis* 2010;**201 Suppl 2**:S85–87.

Gottlieb SL, Xu F, Brunham RC. Screening and treating *Chlamydia trachomatis* genital infection to prevent pelvic inflammatory disease: interpretation of findings from randomized controlled trials. *Sex Transm Dis* 2013;**40**:97–102.

Gussmann J, Al-Younes HM, Braun PR, *et al*. Long-term effects of natural amino acids on infection with *Chlamydia trachomatis*. *Microb Pathog* 2008;**44**:438–47.

Hackstadt TTW, Caldwell HD. Disulfide-mediated interactions of the chlamydial major outer membrane protein: role in the differentiation of chlamydiae? *J Bacteriol*. 1985;**161**:25–31.

Harper A, Pogson CI, Jones ML, *et al*. Chlamydial development is adversely affected by minor changes in amino acid supply, blood plasma amino acid levels, and glucose deprivation. *Infect Immun* 2000;**68**:1457–64.

Hatch TP. Disulfide cross-linked envelope proteins: the functional equivalent of peptidoglycan in chlamydiae? *J Bacteriol* 1996;**178**:1–5.

Herrera VL, Shen L, Lopez LV, *et al*. *Chlamydia pneumoniae* accelerates coronary artery disease progression in transgenic hyperlipidemia–genetic hypertension rat model. *Mol Med* 2003;**9**:135–42.

Hsieh CY, Hsu MJ, Hsiao G, *et al*. Andrographolide Enhances nuclear factor-κB subunit p65 Ser536 dephosphorylation through activation of protein phosphatase 2A in vascular smooth muscle cells. *J Biol Chem* 2011;**286**:5942–5955.

Hybiske K, Stephens RS. Mechanisms of host cell exit by the intracellular bacterium *Chlamydia*. *Proc Natl Acad Sci USA* 2007;**104**:11430–35.

Jayakumar T, Hsieh C-Y, Lee J-J, *et al*. Experimental and clinical pharmacology of *Andrographis paniculata* and its major bioactive phytoconstituent andrographolide. *vid Based Complement Alternat Med* 2013;**2013**:16.

Kalan L, Wright GD. Antibiotic adjuvants: multicomponent anti-infective strategies. *Expert Rev Mol Med* 2011;**13**:e5.

Lee KC, Chang HH, Chung YH, Lee TY. Andrographolide acts as an anti-inflammatory agent in LPS-stimulated RAW264.7 macrophages by inhibiting STAT3-mediated suppression of the NF-kappaB pathway. *J Ethnopharmacol* 2011;**135**:678–84.

Ma L, Liu X, Liang H, *et al*. Effects of 14-alpha-lipoyl andrographolide on quorum sensing in *Pseudomonas aeruginosa*. *Antimicrob Agents Chemother* 2012;**56**:6088–94.

Matsumoto AIH, Miyashita N, Ohuchi M. Plaque formation by and plaque cloning of *Chlamydia trachomatis* biovar trachoma. *J Clin Microbiol* 1998;**36**:3013–9.

Moulder JW. Interaction of chlamydiae and host cells *in vitro*. *Microbiol Rev* 1991;**55**:143–90.

Nguyen BD, Cunningham D, Liang X, *et al*. Lipooligosaccharide is required for the generation of infectious elementary bodies in *Chlamydia trachomatis*. *Proc Natl Acad Sci USA* 2011;**108**:10284–9.

Nugroho AE, Rais IR, Setiawan I, *et al*. Pancreatic effect of andrographolide isolated from *Andrographis paniculata* (Burm. f.) Nees. *Pak J Biol Sci* 2014;**17**:22–31.

Ossewaarde JM, de Vries A, Bestebroer T, *et al*. Application of a Mycoplasma group-specific PCR for monitoring decontamination of Mycoplasma-infected *Chlamydia* sp. strains. *Appl. Environ. Microbiol.* 1996;**62**:328–31.

Patton DL, Sweeney YTC, Stamm WE. Significant reduction in inflammatory response in the macaque model of chlamydial pelvic inflammatory disease with azithromycin treatment. *J Infect Dis* 2005;**192**:129–35.

Peterson EM, Markoff BA, Schachter J, *et al*., The 7.5-kb plasmid present in *Chlamydia trachomatis* is not essential for the growth of this microorganism. *Plasmid* 1990;**23**: 144–8.

Rampioni G, Leoni L, Williams P. The art of antibacterial warfare: deception through interference with quorum sensing-mediated communication. *Bioorg Chem* 2014;**55**:60–68.

Rasmussen SJ, Eckmann L, Quayle AJ, *et al*. Secretion of proinflammatory cytokines by epithelial cells in response to *Chlamydia* infection suggests a central role for epithelial cells in chlamydial pathogenesis. *J Clin Invest* 1997;**99**: 77–87.

Rockey DD, Grosenbach D, Hruby DE, *et al*. *Chlamydia psittaci* IncA is phosphorylated by the host cell and is exposed on the cytoplasmic face of the developing inclusion. *Mol Microbiol* 1997;**24**:217–28.

Slepenkin A, Enquist PA, Hagglund U, *et al*. Reversal of the antichlamydial activity of putative type III secretion inhibitors by iron. *Infect Immun* 2007;**75**:3478–89.

Srivastava PBA, Jha HC, Vardhan H, Jha R, Singh LC, Salhan S, Mittal A. Differing effects of azithromycin and doxycycline on cytokines in cells from *Chlamydia trachomatis*-infected women. *DNA Cell Biol* 2012;**31**:392–401.

Stirling P, Richmond SJ. Production of outer membrane blebs during chlamydial replication. *FEMS Microbiol Lett* 1980;**9**:1574–6968.

Wang Y, Kahane S, Cutcliffe LT, *et al*. Development of a transformation system for *Chlamydia trachomatis*: restoration of glycogen biosynthesis by acquisition of a plasmid shuttle vector. *PLoS Pathog* 2011;**7**:e1002258.

Wiart C, Kumar K, Yusof MY, *et al*. Antiviral properties of ent-labdene diterpenes of *Andrographis paniculata* nees, inhibitors of herpes simplex virus type 1. *Phytother Res* 2005;**19**: 1069–70.

Wolf K, Betts HJ, Chellas-Gery B, *et al*. Treatment of *Chlamydia trachomatis* with a small molecule inhibitor of the Yersinia type III secretion system disrupts progression of the chlamydial developmental cycle. *Mol Microbiol* 2006;**61**:1543–55.

Wyrick PB. *Chlamydia trachomatis* persistence in vitro: an overview. *J Infect Dis* 2010;**201 Suppl 2**:S88–95.

Yilma AN, Singh SR.Morici M., *et al*. Flavonoid naringenin: a potential immunomodulator for *Chlamydia trachomatis* inflammation. *Mediators Inflamm* 2013.

Zaidan MR, Noor Rain A, Badrul AR, *et al*. *In vitro* screening of five local medicinal plants for antibacterial acivity using disc diffusion method. *Trop Biomed* 2005;**22**:165–70.

Zheng Y, Liu X, Guo SW. Therapeutic potential of andrographolide for treating endometriosis. *Hum Reprod* 2012;**27**:1300–13.

Zhou H, Huang Q, Li Z, *et al*. pORF5 plasmid protein of Chlamydia trachomatis induces MAPK-mediated pro-inflammatory cytokines via TLR2 activation in THP-1 cells. *Science China Life Sciences* 2013;**56**:460–66.

Zigangirova NA, Zayakin ES, Kapotina LN, *et al*. Development of chlamydial type III secretion system inhibitors for suppression of acute and chronic forms of chlamydial infection. *Acta Naturae* 2012;**4**:87–97.